

Numerical Validation and Analysis of the Semi-submersible Platform of the DeepCwind Floating Wind Turbine based on CFD

Ke Xia, Decheng Wan*

State Key Laboratory of Ocean Engineering, School of Naval Architecture, Ocean and Civil Engineering, Shanghai Jiao Tong University, Collaborative Innovation Center for Advanced Ship and Deep-Sea Exploration, Shanghai 200240, China

*Corresponding author, E-mail: dcwan@sjtu.edu.cn.

Abstract

With the rapid development of the ocean engineering and the renewable energy, more and more attention are paid to the floating wind turbine. In recent years, researchers do much work on the floating wind turbine while most of the researchers investigate the problem by experiment or 3D potential theory but not the CFD, which has its own advantages in some aspects. A numerical simulation of motion performance of the DeepCwind floating wind turbine is investigated in the present study. In this paper, motion responses of the platform with mooring system under regular wave conditions are investigated numerically by a viscous flow solver naoe-FOAM-SJTU based on the open source toolbox OpenFOAM.

The motion performance of the platform under five different regular wave conditions are presented and compared with the data of the model test to validate the accuracy of the solver. The motion curves are presented in both the time domain and the frequency domain to research the response characteristics of the platform. Subsequently, the investigation about the parameter sensitive is conducted, and the results indicate that the motion performance would be better with the decrease of the height of COG and the increase of the draft within a reasonable range. And the broken mooring line has a huge impact on the platform to which should be pay more attention for the safety of the platform.

Keywords: semi-submersible platform, motion performance, parameter sensitive, naoe-FOAM-SJTU solver.

Introduction

As to the energy crisis and the environmental issues like pollution and global warming, the exploration for renewable and clean energies becomes crucial. Some potential resources become more and more significant, just like the wind, wave, solar and tidal, that numerous researchers are devoted to them (Ma and Hu, 2014) [1]. The wind energy is the fastest growing renewable energy resource which can never be exhausted, so it's attracting more and more attention worldwide (Tang and Song, 2015) [2].

As the main part of the floating wind turbine, the motion performance of the floating platform is significant for the wind turbine, and the motion performance of the platform has obvious effects on the aerodynamic performance of the wind turbine as well as the electricity generating capacity (Zhao and Yang, 2016) [3]. One challenge of the floating wind turbines is the wave induced platform tilt motion, which will heavily increase the displacements and load on turbine structure due to high inertial and gravitational forces and will bring severe fatigue and ultimate loads at tower bottom and blades roots (Hu and He, 2015) [4].

To research the motion performance and the wave loads of the floating platform, predecessors have done much work. A reasonable assumption is put forward by Hooft (2002) [5] that

Morison equation can be used to calculate the wave force of the platform, which is a semi empirical formula and wave force around the platform can be divided into two parts, one is inertia force and the other one is drag force. This formula is widely used in the calculation of small scale component of the platform whose cross section is relatively simple (Lee and Incecik, 2005) [6]. Frank (2005) [7] find that the pulse source can be discretely distributed on the surface of the floating structure, so that people can calculate the wave force of the floating structure with arbitrary cross section shape, which is superior to the Morison equation, and this method is suitable for the compiling of the program. In the recent research about the hydrodynamic performance of the floating platform. Nowadays, most of the researchers investigate the motion response of the platform in the wave environment by the 3d potential theory. In this theory, platform is solved as a whole part not several sections, and the surface of the physical model of the platform below the waterline will be replaced by the mesh model so that the Green function can be got to calculate the velocity potential, and the distribution of the wave pressure can be calculated, as well as the motion response (Shi and Yang, 2010) [8]. At present, most popular hydrodynamic software such as AQWA, Seasam, Hydrostar and FAST are all based on the 3d potential theory to do the hydrodynamic calculation of the platform (Shi and Yang, 2011) [9]. 3D potential theory has several advantages that the calculated results are relatively accurate when compared with the results of the experiment, and it is very convenient which can get a satisfactory statistical results in a short period of time. However, the disadvantages of this method is extremely obvious. 3d potential theory is based on an assumption that the water is potential flow which is non-viscous, irrotational and incompressible. This is a simplification of the actual phenomenon which leads to obvious error from the results of the experiment. Actually, the viscosity of the water shouldn't be ignored in the motion of the platform, for it has significant effect on the motion of response, especially when the period of the coming wave is close to the natural period of the platform. Also the potential theory can't deal with a strongly nonlinear problem (Wang and Cao, 2015) [10]. On the contrary, Computational Fluid Dynamics (CFD) methods might be employed to obtain a better result via employing a more realistic model. The most prominent advantage of the CFD is that result of the simulation is more authentic and with the consideration of viscous flow, some more complex problems can be simulated such as green water, slamming, wave run up and other strongly nonlinear issues, which can't be solved by the potential flow method (Liu and Wan, 2015) [11]. In this paper, a viscous flow solver (naoe-FOAM-SJTU) (Shen and Wan, 2013; Zhou and Wan, 2013; Cao and Wan, 2014; Zha and Wan, 2014; Zhao and Wan, 2015) [12] which is developed and based on the popular open source toolbox OpenFOAM for predicting dynamics of floating structures with mooring systems is presented. The solver is adopted to study motion responses of a floating semi-submersible platform with mooring system under regular wave conditions.

The outline of this paper is as follows. Mathematical equations and numerical methods are first described concerning fluid flow, floating platform and mooring systems. Parameters of the platform and mooring system studied here together with computational domain are then presented. Then the validation work is done to compare the calculated results with the data of the model test which is conducted by the University of Maine DeepCwind program at Maritime Research Institute Netherlands' offshore wind/wave basin, located in the Netherlands (Robertson, 2012) [13]. Also, the calculation result of the same issue simulated by the FAST which is a software who is based on the 3d potential flow theory is added to the comparison (Alexander, 2013) [14]. The floating wind turbine used in the tests was a 1/50th-scale model of the NREL 5-MW horizontal-axis reference wind turbine with a 126 m rotor diameter. Subsequently, the research of parameter sensitive is done to investigate the effect of different height of the gravity center and draft on the motion performance of the platform. In

addition, the mooring line may be broken when the wave or wind is too large, so one of the mooring line is removed in this paper to study the motion response of the platform in a dangerous condition. Results and conclusions are made at the end.

Methods

The present solver naoe-FOAM-SJTU adopted for numerical simulation is based on a built-in solver in OpenFOAM named interDyFoam, which can be used to solve two-phase flow which is incompressible, isothermal and immiscible. To deal with common fluid-structure interaction problems in ship hydrodynamics and offshore engineering, several modules are further developed and integrated into the solver, such as a wave generation/damping module, a six-degrees-of-freedom (6 DOF) module and a mooring system module. Laminar Reynolds model are carried out in all the calculations. Mathematical formulae related to the solver are described as follows in detail.

1. Governing equations

For transient, incompressible and viscous fluid, flow problems are governed by Navier-Stokes equations:

$$\nabla \cdot \mathbf{U} = 0 \quad (1)$$

$$\frac{\partial \rho \mathbf{U}}{\partial t} + \nabla(\rho(\mathbf{U} - \mathbf{U}_g)\mathbf{U}) = -\nabla p_d - \mathbf{g} \cdot \mathbf{x} \nabla \rho + \nabla(\mu \nabla \mathbf{U}) + \mathbf{f}_\sigma \quad (2)$$

Where \mathbf{U} and \mathbf{U}_g represent velocity of flow field and grid nodes separately; $p_d = p - \rho \mathbf{g} \cdot \mathbf{x}$ is dynamic pressure of flow field by subtracting the hydrostatic part from total pressure p ; \mathbf{g} , ρ and μ denote the gravity acceleration vector, density and dynamic viscosity of fluid respectively; \mathbf{f}_σ is surface tension which only takes effect at the free surface and equals zero elsewhere. The Laminar model means that the Navier-Stokes equation will be solved directly and the turbulence model is not been considered in the calculation.

2. Wave generation/damping

For a floating platform, wave loading is a most important environment loads. So that, wave generation must be implemented numerically. The wave generation module of the naoe-FOAM-SJTU can make various types of waves such as linear wave and Stokes 2nd order waves which will be adopted in the following paper. The linear wave (3) and Stokes 2nd order wave theory (4) are adopted in this paper and the equation used to describe free surface is:

$$\eta = A \cos \theta \quad (3)$$

$$\eta = a_1 \cos(kx - \omega t) + a_2 \cos 2(kx - \omega t) \quad (4)$$

Where A and $H=2A$ denote wave amplitude and wave height; a_1 is the amplitude of the first order item and the a_2 is the amplitude of the 2nd order item.

Once the wave is generated, reflection has to be considered when wave propagates towards outlet boundary which will travels in an opposite direction that will interfere the incident wave. So that, the wave damping module is developed in this solver. Sponge layer takes effect by adding an additional artificial viscous term to the source term of the momentum equation. The new term is expressed as:

$$\mathbf{f}_s = -\rho \mu_s \mathbf{U} \quad (5)$$

Where μ_s is the artificial viscosity calculated by the following equation:

$$\mu_s(x) = \begin{cases} \alpha_s \left(\frac{x-x_0}{L_s} \right)^2, & x > x_0 \\ 0, & x \leq x_0 \end{cases} \quad (6)$$

Where α_s is a dimensionless quantity defining damping strength for the sponge layer. Other parameter can be easily understood by reading the following figure.

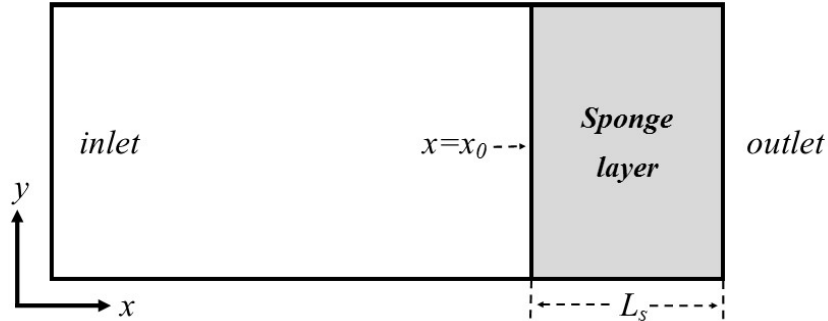


Figure 1. Overlooking of the calculation domain and sponge layer

3. Mooring system

To simulate the actual condition and the interaction problem of the mooring line and floating platform, the code of mooring line module is developed and added to the existing solver. The mooring line used in this paper is based on the PEM (piecewise extrapolating method) which is implemented to calculating the statics of mooring lines and it could take into account line elongation as well as the drag force induced by the fluid. With this method, mooring lines are divided into a number of segments, and a typical example of these is shown in Figure 2. Equations of static equilibrium are established in both horizontal and vertical directions:

$$\begin{cases} T_{xi+1} = T_{xi} + F_i ds \cos \varphi_{i+1} + D_i ds \sin \varphi_{i+1} \\ T_{zi+1} + D_i ds \cos \varphi_{i+1} = T_{zi} + F_i ds \sin \varphi_{i+1} + w_i dl \end{cases} \quad (7)$$

Where T_x , T_z and φ represent horizontal and vertical components of tension at a cross section of one segment and the angle between tension and T_x ; dl and ds are length of the segment before and after elongation respectively; w is net submerged weight of lines per unit length; D and F denote normal and tangential components of drag force acting on the segment which are calculated by Morison's equation.

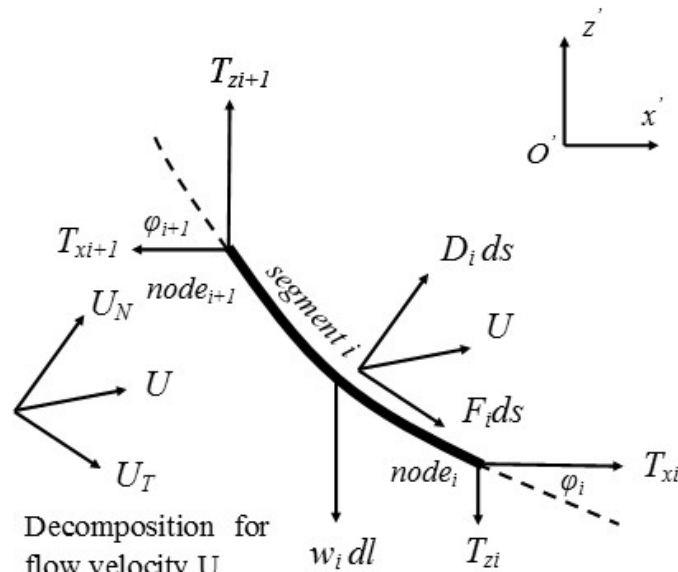


Figure 2. Force analysis of a mooring line segment for PEM

Computational model

A deep water semi-submersible platform of the DeepCwind with a catenary mooring system is presented in this paper, which is investigated both experimentally and numerically by Alexandwer (2012). Parameter of this platform and mooring system are respectively given in the section 1 and 2, as well as the computational domain.

1. Platform parameter

This floating platform for this model is semi-submersible which is downloaded from the website of National Renewable Energy Laboratory (NREL). It's standard mode named OC4 that researchers all over the world are investigating it. The platform is made up of three offset columns with larger diameter lower bases, one center support column for the turbine and a series of horizontal and diagonal cross bracing, and for the purpose of simplify the calculation, the diagonal cross bracing which is not very important in the seakeeping calculation is removed. The drawing of the DeepCwind semi-submersible platform are given in Figure 3 and the gross properties are presented in the Table 1. Furthermore, the Figure 4 give out the coordinate system of the platform in this study.

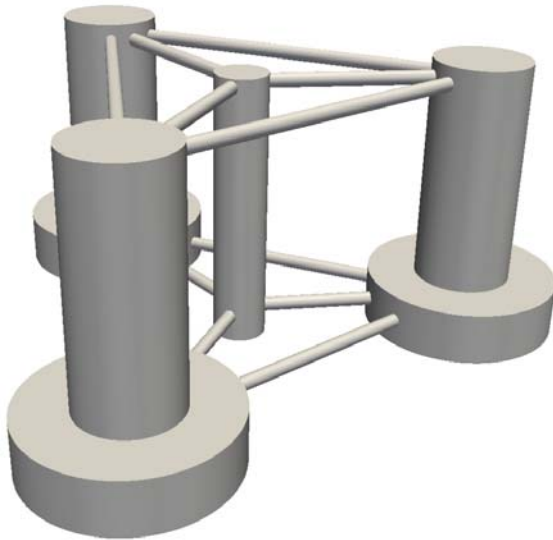


Figure 3. Overlooking of the 3d model platform

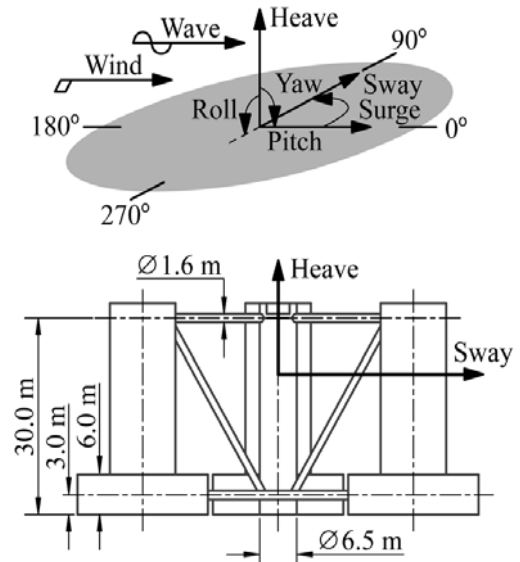


Figure 4. Coordinate system of the platform

2. Mooring system configuration

The mooring system of this semi-submersible platform is composed of 3 lines which interval between adjacent mooring lines is 120 degrees. And the fairleads of all lines are positioned at the surface of the base column. And the arrangement of the mooring system is shown in the Figure 5. And the parameter of the mooring system is presented in the Table 2.

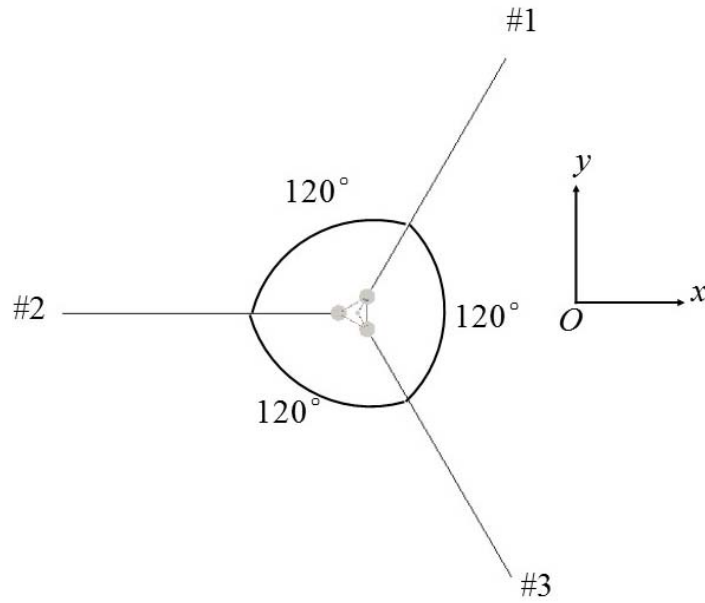


Figure 5. Configuration of the mooring system and platform

Table 1. Gross parameters of the semi-submersible platform of DeepCwind

Primary parameter	Unit	Value
Depth of platform base below SWL (total draft)	m	20
Elevation of main column (tower base) above SWL	m	10
Elevation of offset columns above SWL	m	12
Spacing between offset columns	m	50
Length of upper columns	m	16
Length of case columns	m	6
Depth to top of base columns below SWL	m	14
Diameter of main column	m	6.5
Diameter of offset (upper) columns	m	12
Diameter of base columns	m	24
Diameter of pontoons and cross braces	m	1.6
Displacement	m ³	13986.8
Center of mass location below SWL along platform center line	m	9.936

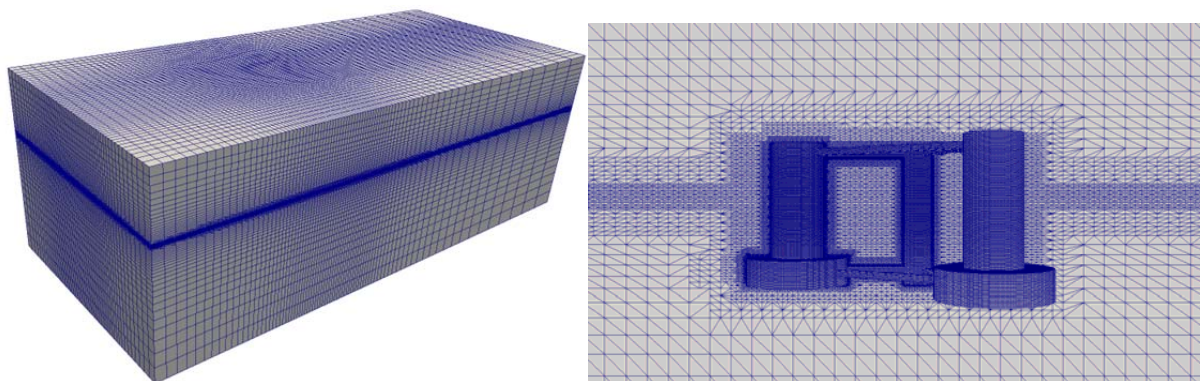
Table 2. Primary parameters of the mooring system

Primary parameter	Unit	Value
Number of mooring lines		3
Angle between adjacent lines	°	120
Depth to anchors below SWL (water depth)	m	200

Depth to fairleads below SWL	m	14
Radius to fairleads from platform centerline	m	4.0868
Radius to anchors from platform centerline	m	837.6
Equivalent mooring line mass in water	kg/m	108.63
Equivalent mooring line extensional stiffness	N	7.536E+8

3. Calculation domain

The solver used in this paper is based on the OpenFOAM who provides users a very powerful and convenient utility named snappyHexMesh (OpenFOAM, 2013) [15] to create the computational mesh with high quality in relatively short time. The overview of the computational mesh is shown in the Figure 6 (a), and the local refinement of the mesh near the platform is given in the Figure 6 (b). The model is located in the center of the computational domain. The totally cell number is about 1.3 million. And the principal dimension of the calculation domain is shown in the Figure 7.



(a) Overview of all the mesh

(b) Local view near the platform

Figure 6. Computational mesh of the platform

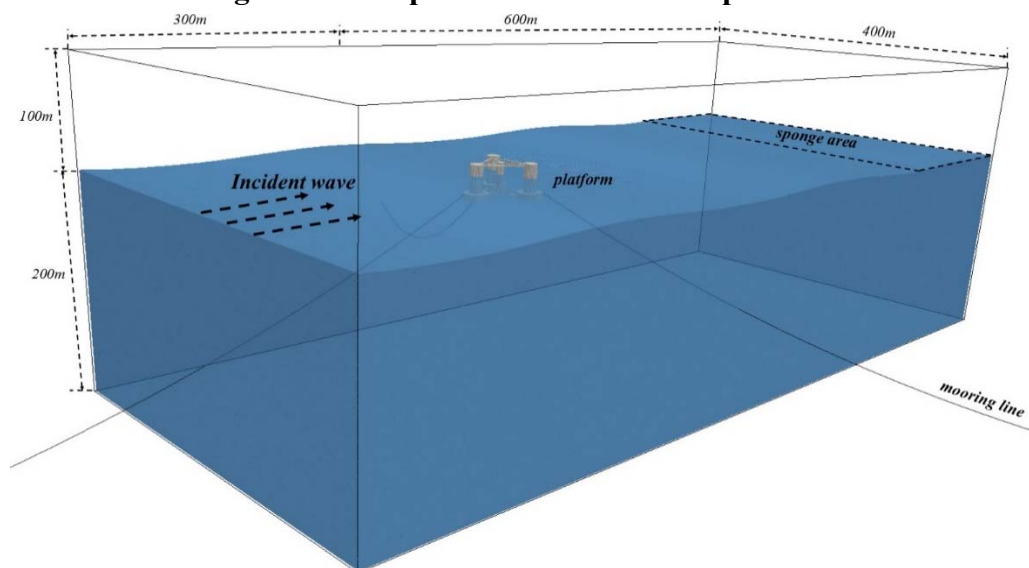


Figure 7. Overview of the calculation domain with principle dimension

Validation

The follow research are all based on the solver naoe-FOAM-SJTU which is composed of a wave generation module, 6dof motion module, mooring system module and wave damping module. With these powerful module, several research can be done such as the problem of ship hydrodynamics and offshore engineering in various condition. But before doing the research about the platform of the DeepCwind, the validation work should be done to verify the correctness of the solver. So that, the validation work is done to compare the calculated results with the experimental data which is conducted by the Maritime Research Institute Netherlands' offshore wind/wave basin. The response of the DeepCwind semi-submersible platform to regular waves in the absence of wind is investigated in the validation of this paper. Different regular waves are considered, the amplitudes and periods of which are given in the Table 3. All waves propagated in the positive surge direction. It should be noted that two distinct amplitudes were investigated for periods of 14.3 and 20.0 s for the purpose of assessing any nonlinearity in system response. The motion performance of the DeepCwind platform is characterized by response amplitude operators (RAOs) magnitudes, which normalize the amplitude of a periodic response of a field variable by the amplitude of the regular waves.

Since the wind is not considered in this study, the weight, height of gravity and the moment of inertia of the whole wind turbine are converted and added to the parameters of the platform. Before the calculation of the motion, the work of wave generation should be done in the empty computational domain without the platform. The wave probe is set at the longitudinal min-section of the domain near the inlet. And the elevation of the wave whose wave height is 5.15 m and the period is 12.1 s is shown in the Figure 8 (a). The time step used is fixed at 0.05s and the overall time simulated is set as 300s. Figure 8 (b), (c) and (d) shows the surge, heave and pitch response of the platform within the wave whose height is 5.15 m and the period is 12.1 s. For the limitation of the length of the paper, the waveform figure of other waves and the motion response of the platform under other wave conditions are not given in the paper.

Table 3. Calculated regular wave amplitudes and natural periods

Amplitude (m)	Period (s)
3.57	14.3
3.79	20
5.15	12.1
5.37	14.3
5.56	20

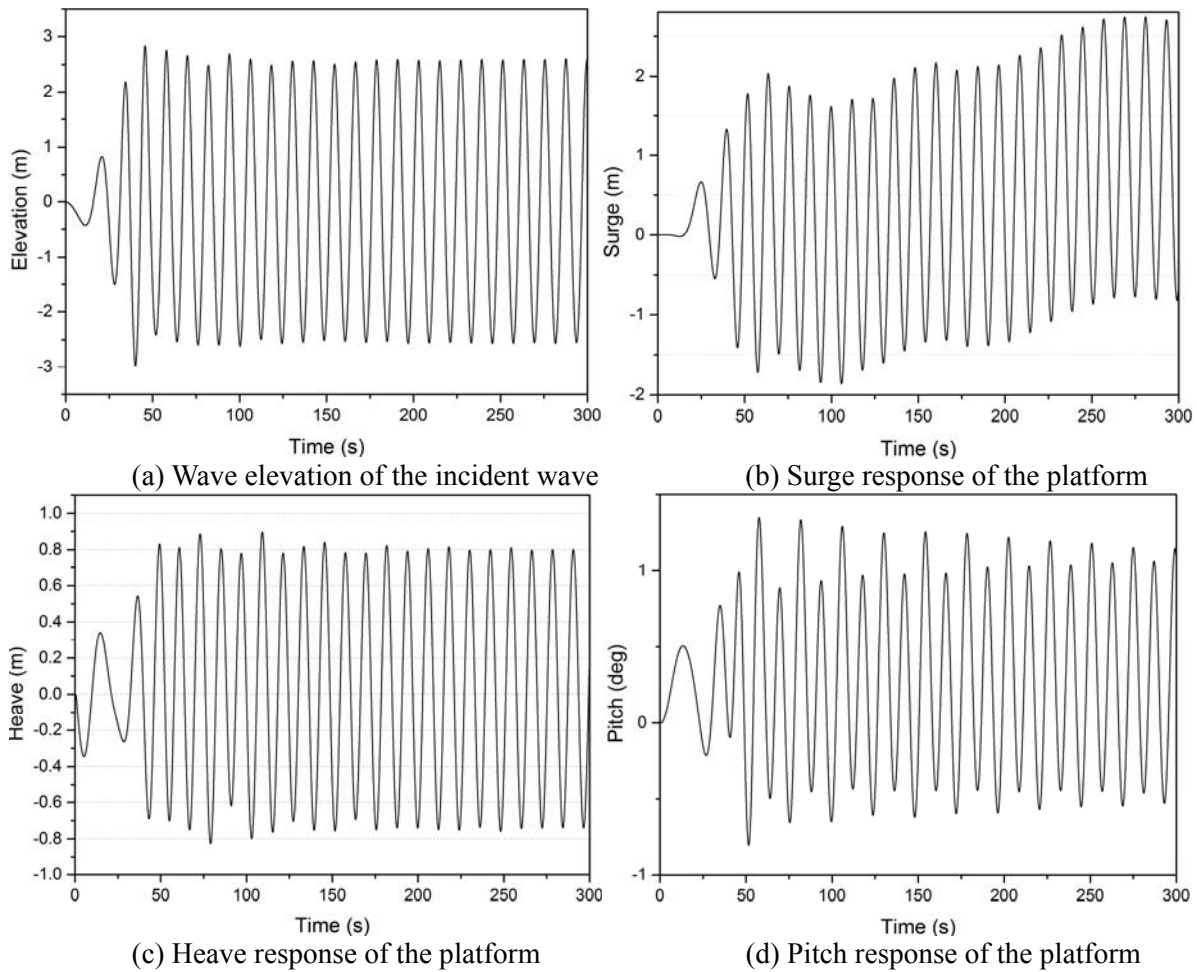


Figure 8. Elevation of the incident wave and motion response of the platform

Since the platform is calculated in the regular waves and according to the International Towing Tank Conference (ITTC) that motion data should be collected at least for 10 quasi-steady cycles under regular wave conditions to ensure accuracy of results (ITTC, 2002) [16]. So that in this paper, the last ten period of the motion response are considered and calculated the average value. And then the RAO, the average amplitude of the motion response divided by the wave amplitude, can be counted.

Before showing the validation result, it is a wonderful job to analyze the motion response results given in the Figure 8, whose incident wave height is 5.15 m. It's evident that the height of the made wave highly agree with the requested wave and it's very steady after 100s. Therefor the following analysis can be based on the 100-300 s of the calculation. The average surge amplitude is 1.73 m, and the average heave amplitude is 0.78 m. In addition, the average pitch amplitude is 0.83° . From the figure above, several conclusion can be drawn.

Firstly, it's evident that the surge motion of the platform is nonlinear, and under the action of the wave force, the platform drifts about 1 m along the direction of the wave during 300 s. Subsequently, the heave response is relatively steady that it's almost a linear motion. Finally, a conclusion can be drawn that the pitch motion natural period of the platform is definitely larger than the period of incident wave which is 12.1 s, because it's obvious that the amplitude of the pitch motion of the platform presents a periodic variation, one large and one small, which means that in the motion of the platform, the second wave acts on the platform before the first natural period of the pitch motion over, and then causes the phenomenon of nonlinear pitch motion, as well as the increased pitch motion center. After the following study, it is

found that the nonlinear phenomenon is gradually stabilized after 350 s, and the average pitch displacement is about 0.25° instead of 0° .

The RAO magnitude for surge, heave and pitch are given in the Figure 9 for the five regular waves investigated, and the comparison is conducted between the experiment, naoe-FOAM-SJTU and FAST. FAST is a professional software for calculation of performance of wind turbine, who is based on the 3d potential theory, and the calculation with FAST is conducted by Alexander (2013).

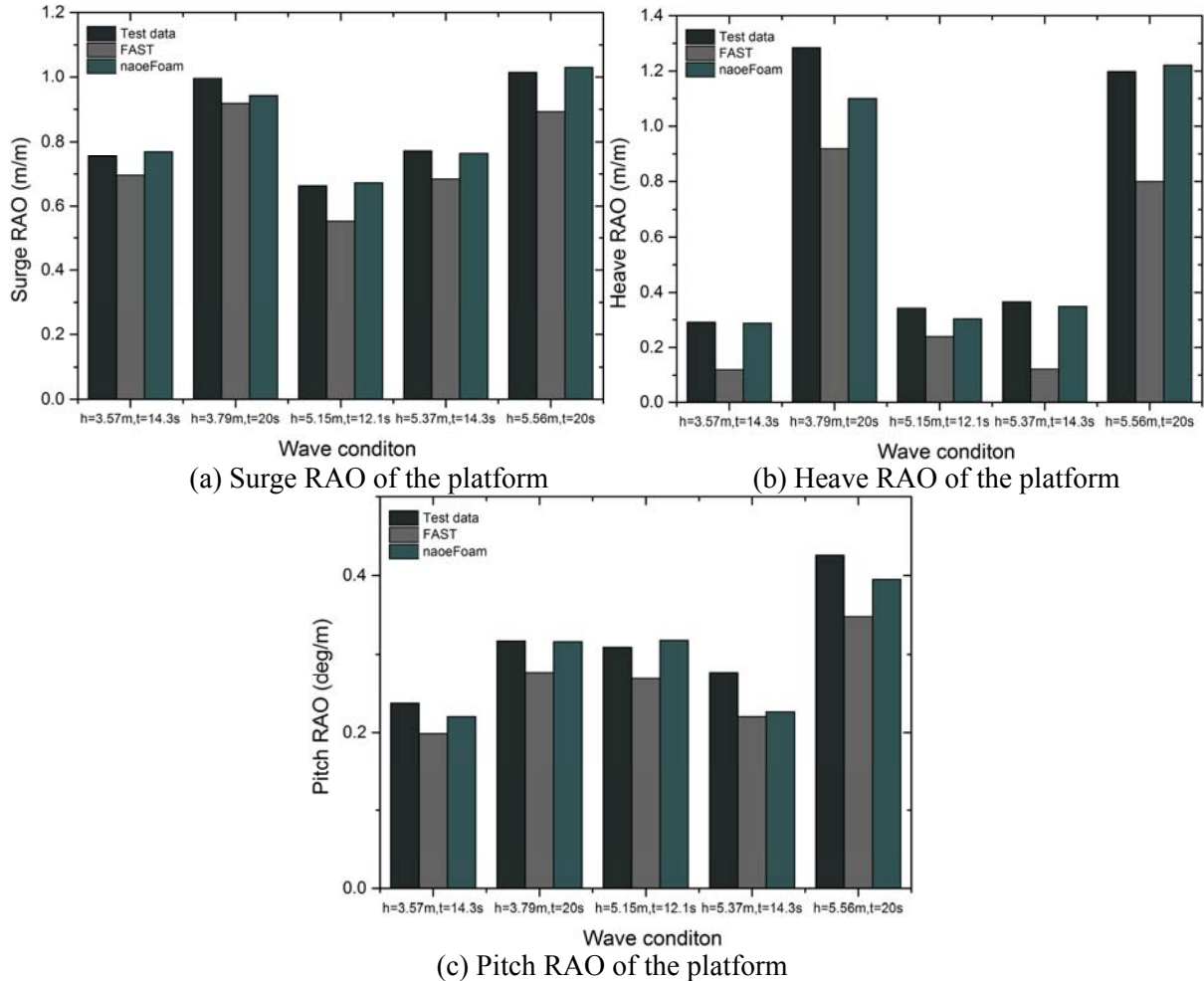


Figure 9. Comparisons of RAOs from experimental test, FAST and naoe-FOAM-SJTU

Almost all the comparisons in the Figure 9 between the test data and the solver that used in this paper are extraordinarily good, which is much better than the FAST in these comparisons. The large discrepancy is likely a result of the damping system that the quadratic damping model employed in the FAST, which over-predicts the damping in large amplitude heave scenarios at the expense of properly modeling the damping for small to moderate motions. The first conclusion can be drawn that the response of the platform to the low frequency wave is more intense that the RAOs of the wave condition whose period is 20 s are obviously larger than that of 12.1s and 14.3 s. At the same time, another conclusion can be concluded from the Figure 9 that there exists nonlinear phenomenon in the test and calculation that the RAOs of the platform are exactly different from each other with the dame wave period but distinct wave height which should be the same regardless of the viscosity.

As everybody knows, there is no viscosity and vortex in the 3d potential theory, so in the calculation with FAST, it is difficult to confirm a right damping coefficient. However, it is precisely the advantage of CFD, which is based on the Navier-Stokes equations so that the viscosity and vortex are take into consideration. As shown in the Figure 10, it present the vortex and the radiation or reflected wave generated in the procedure of motion of the platform under the 5.37 m wave height condition. Moreover, CFD can do some nonlinear problems, such as the wave run up and fracture in the process of calculation, which is more close to the actual situation. Therefore, the solver used in this paper is validated.

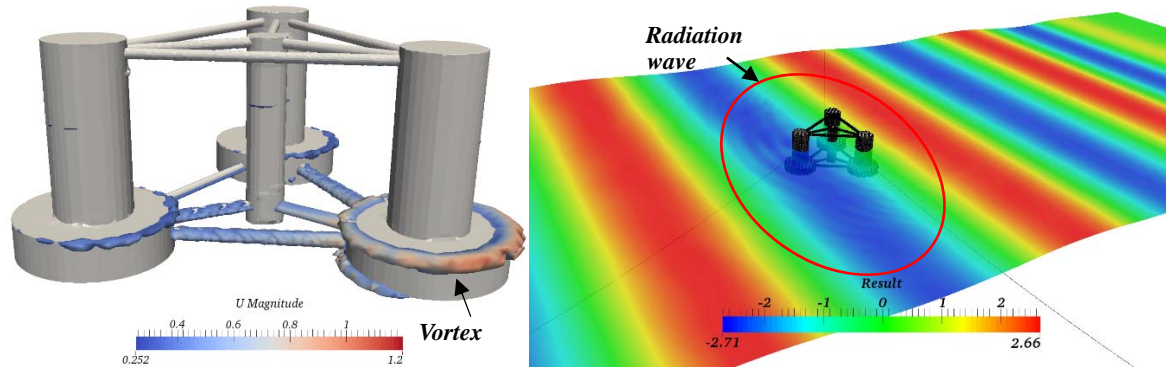


Figure 10. Vortex and radiation wave generated by the motion response of the platform

Results

In order to evaluate the influence of the parameter sensitive on the motion response and other hydrodynamic parameters. And through the investigation, several laws can be drawn to get the best motion performance of the platform in the design procedure to ensure the stability of electricity generating of the wind turbine. Following three aspects are investigated: 1. The research about the effect of different height of gravity center of the platform on the motion performance of the platform. 2. The influence of different draft of the platform on the performance of the platform. 3. A dangerous condition of the platform is considered that one mooring line is removed to investigate the influence on the motion performance of the platform.

1. Effect of height of gravity center

The height of gravity center is a vital parameter for an offshore platform, and it directly affects the stability of the platform. At the same time, the gravity height will exactly affect the sea-keeping performance of the platform by affecting both the motion period and the motion amplitude. Therefore, in this section, three distinct height of COG (center of gravity) is considered, which includes the original height -9.9 m, and the others. The sketch of the distribution of the different COG calculated in this study is shown in the Figure 11.

The 5.15 m wave height and 12.1s wave period wave condition is selected in the investigation of effect of the COG. And in this section, the overtime of calculated condition are set as 200s, which is due to the large amount of computation and aimed to save time. And the comparison of -7m, -13m and the original height -9.9m are given in the Figure 12.

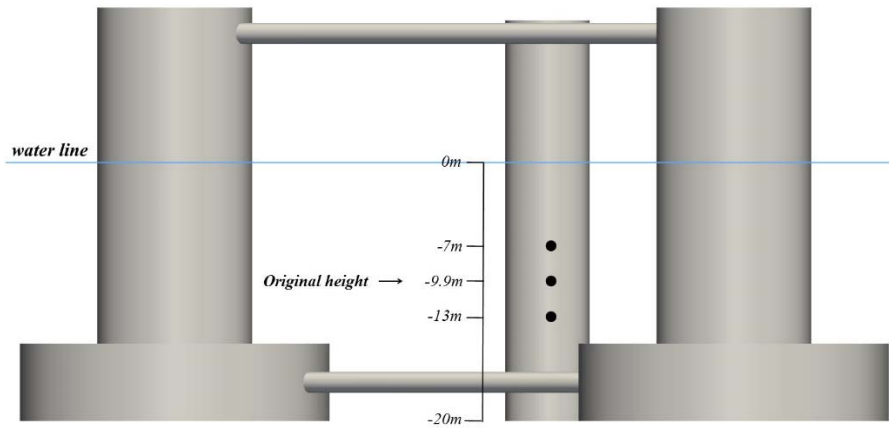
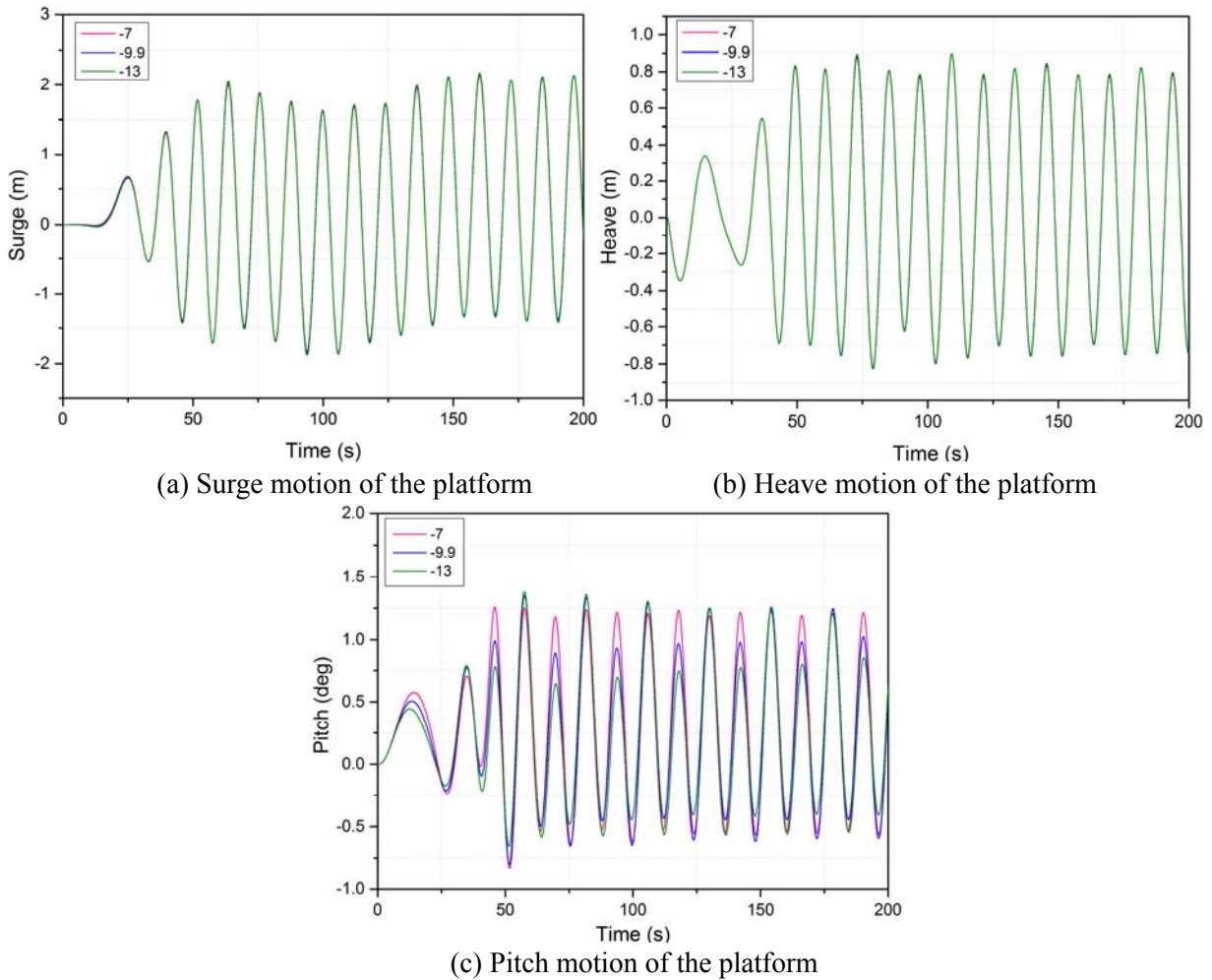


Figure 11. Distribution of the calculated height of gravity center



(a) Surge motion of the platform

(b) Heave motion of the platform

(c) Pitch motion of the platform

Figure 12. Comparison of the effect of different height of COG on the platform

A conclusion can be drawn that the motion performance of the platform is better with the decrease of the height of the COG within a reasonable range. The surge and pitch motions of different height of COG didn't show a significant difference that the surge and heave amplitude of these three height of COG is almost the same. The difference of the pitch motion between the calculated conditions is quite obvious. The first conclusion can be gotten that the pitch performance becomes better with the decrease of the height of the COG. Subsequently, the pitch motion trends are consistent, which follows a similar increase or decrease law and

also the strong nonlinearity is very evident in this process. Moreover, the pitch motion performance is relatively steady than other conditions when the height is -7 m which is almost a linear motion.

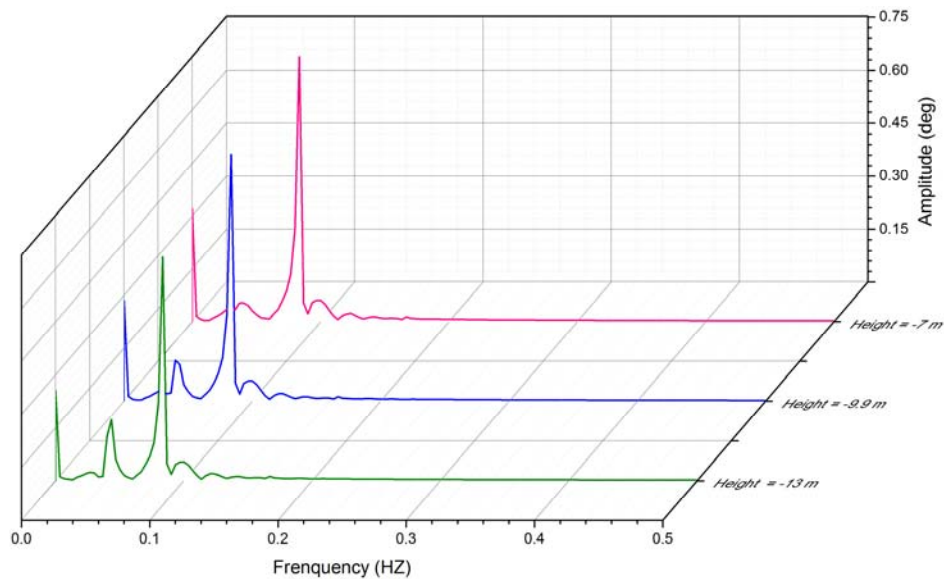


Figure 13. FFT of the pitch motion with different height of COG

For the strong nonlinear pitch motion, the FFT (Fast Fourier Transform) about the motion amplitude is conducted, for the strong nonlinear phenomenon, to investigate the characteristics of the pitch motion performance of the platform on the frequency domain. The results are given in the Figure 13, and to do a further analysis, the specific value about the first order term and the second order term of the amplitude of the pitch motion is given in the Table 4.

Table 4. Specific numerical analysis in frequency domain

Height of COG (m)	Orders	Frequency (HZ)	Amplitude value (deg)
-7	First order	0.083	0.782
	Second order	0.039	0.053
-9.9	First order	0.083	0.710
	Second order	0.040	0.116
-13	First order	0.083	0.654
	Second order	0.043	0.170

By the Table 4, some obvious rules can be summed up that besides the first order motion, there also exists second order pitch motion which can be easily found in the Figure 13. The frequency of the first order motion is about 0.083 HZ which is the frequency of the incident wave. And the frequency of second order of different COG are distinct which is related to the natural period of the platform and the mooring system, for the period of the platform come up from theory say that it is affected by the height of the COG. The frequency of the second order

pitch motion decrease with the COG rise up. And it is also evident that the second order of the pitch motion of the height -7 m is quite small which means that it is nearly a linear motion in this condition. The amplitude of the first order plus that of the second order is almost the amplitude of the pitch motion amplitude of the platform, so that it is easy to find the law of the effect of the COG on the pitch motion of the platform by add the first order's amplitude and the second order one. Then the law mentioned above can be confirmed that the motion performance will be better with the decrease of the height of the COG within a certain range.

2. Effect of draft

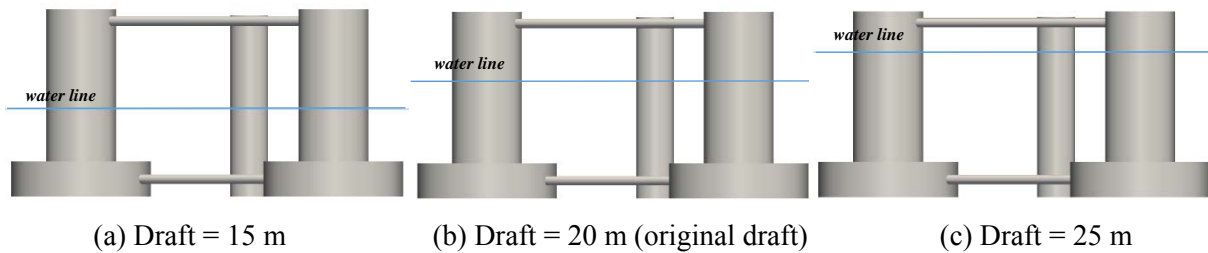


Figure 14. Different draft condition of the platform

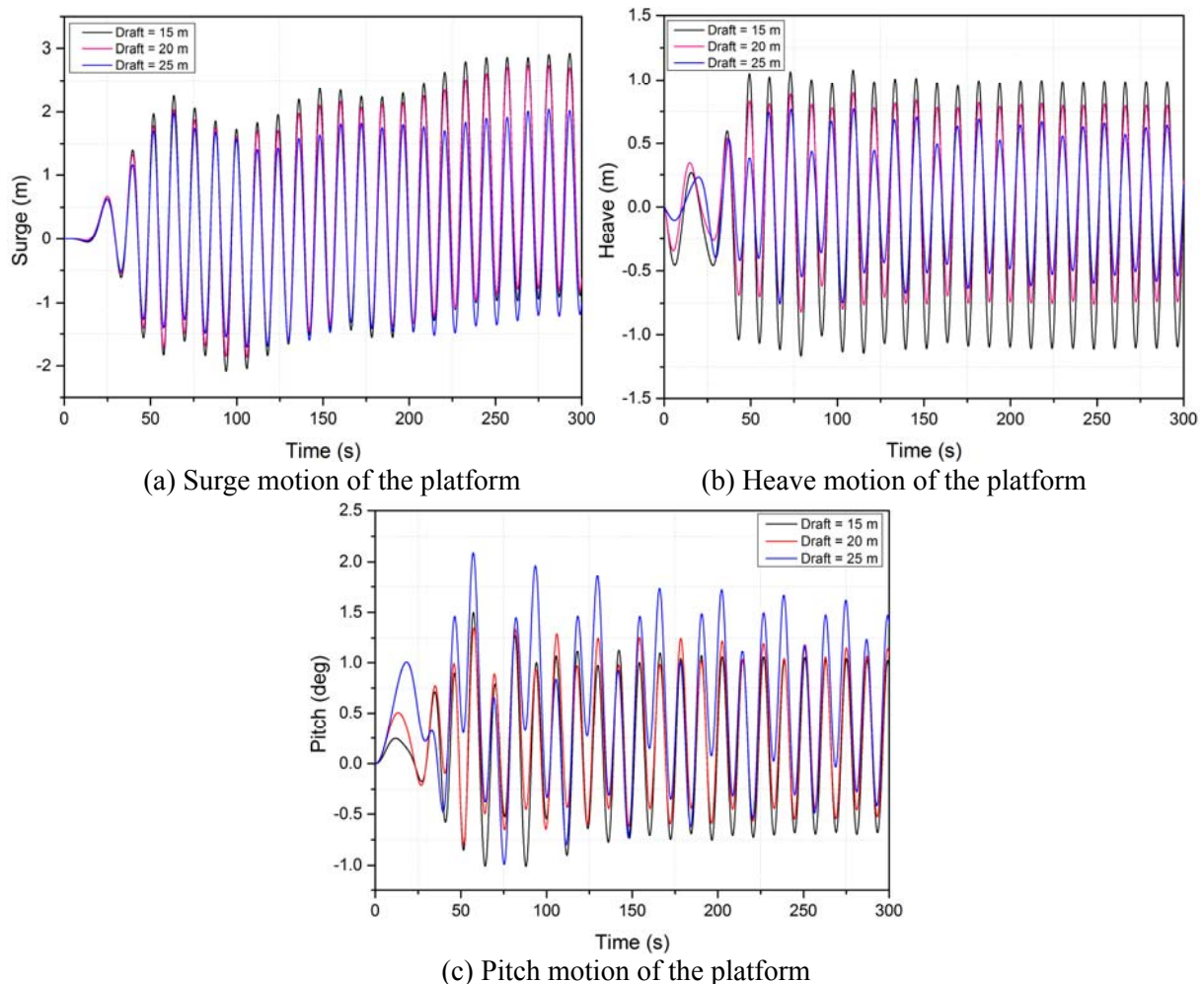


Figure 15. Effect of draft on the motion response of the platform

Draft is also a significant parameter for a floating platform who not only affects the displacement of the hull but also affect the motion performance. And for a platform for the floating wind turbine, the draft would change if the mass or the force that act on the blade

changed, and the draft would be different in different condition. So it is meaningful to investigate the effect of draft on the motion performance of platform. In this section, three different drafts are conducted including 15 m, 25 m and the original one 20 m. The Sketch is given in the Figure 14 and the curves of response results are shown in the Figure 15.

The average motion amplitude of each condition can be calculated easily when the motion are quasi-steady. The three kinds of average motion amplitude of the platform with 25 m draft are that surge amplitude 1.629 m, heave amplitude 0.558 m and the pitch amplitude 0.85° . The average motions amplitude of the platform with 20 m draft are given in the validation that surge 1.73 m, heave 0.78 m and pitch 0.83° . At last, the average motions amplitude of the platform with 15 m draft are that surge 1.925 m, heave 1.043 m and pitch 0.862° . So an evident law can be found from the comparison of the value that the motion performance of the platform is better with the increase of the draft within a reasonable range, which can be easily observed from the Figure 15. Also a strange point can be found after analysis that the pitch motion of the 25 m draft is larger than that of 20 m, which is inconsistent with the rules summed up before and a likely reason for this problem is that it is obvious that the pitch motion of the platform with 25 m draft has obvious oscillation which is not steady for the short calculation time, thus the average value is probably larger than the pitch motion amplitude in the steady condition. The Figure 16 show the motion of the platform with different draft in the same time 295s that platforms reach the motion amplitude. It is easily to find that the motion degree is larger with the draft decrease and it can be also found that the free surface has an obviously nonlinear up and down near the platform.

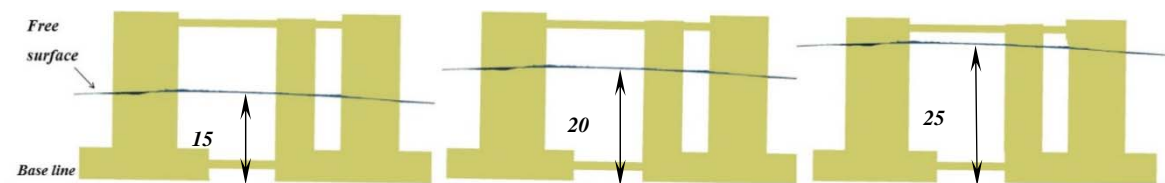


Figure 16. Posture of the platforms with different draft in the 295 s

3. One mooring line broken condition

The mooring system play a vital role in both working and survive condition of the platform, which not only maintains the position of the platform in the horizontal direction but also provides restoring force and conductive to the performance of the platform. In this section, a dangerous condition is investigated that one mooring line, the #3 line, of the mooring system is removed to represent the broken one. The model diagram of the configuration of the mooring system is shown in the Figure 17, and the comparison between this condition and the normal condition is shown in the Figure 18.

As can be seen in the Figure 18, the x-axis direction motion appeared a huge mutation when one mooring line is broken down and the platform moves in negative direction of the x-axis in which the most distance is about 15 m at 50 s and pulling back by the rest lines after that and finally steady at about 6 m against the x-axis. As shown in the Figure 19, which is comparison between the position of the platform at 50 s and the original position of the platform. Subsequently, in the z-axis direction, the platform float up 0.21 m after one mooring line is broken for the lack of pretension force. Finally, in the rotation direction, the platform also has an obvious change on the floating condition which skews about 0.39° overall.

Besides the movement mentioned above, it is also necessary to analyze the surge, heave and pitch motion response of the platform. As shown in the Figure, the surge amplitude of the normal condition is 1.73 m and 1.78 m at the one line broken condition. And the platform in

these two condition presents the same heave and pitch amplitude that heave 0.78 m and pitch 0.83° although the large difference between the displacements of these two kinds of situation.

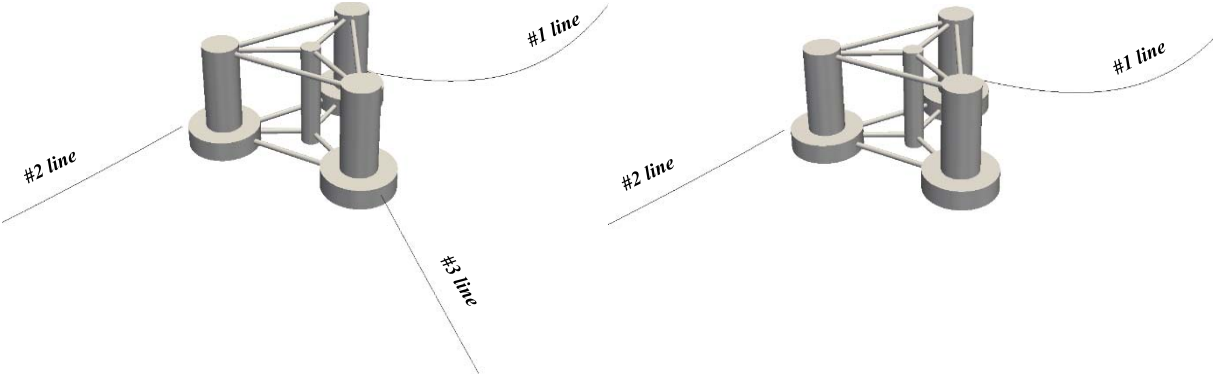


Figure 17. The diagram of complete mooring system and broken mooring system

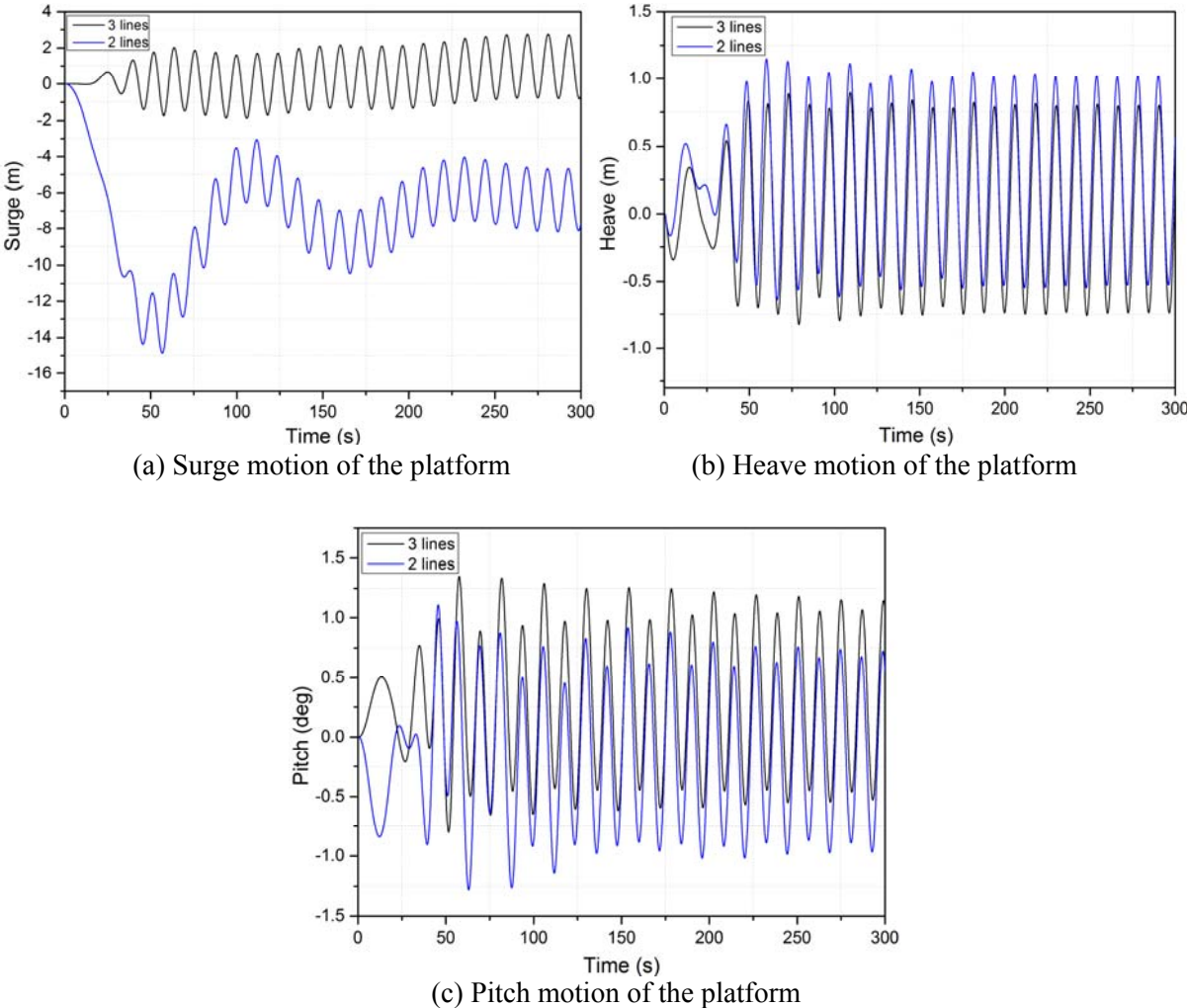


Figure 18. Response of working condition and one mooring line broken condition

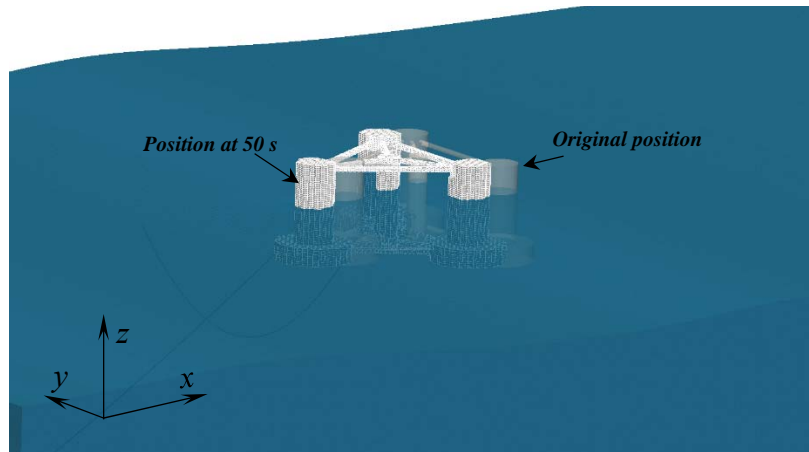
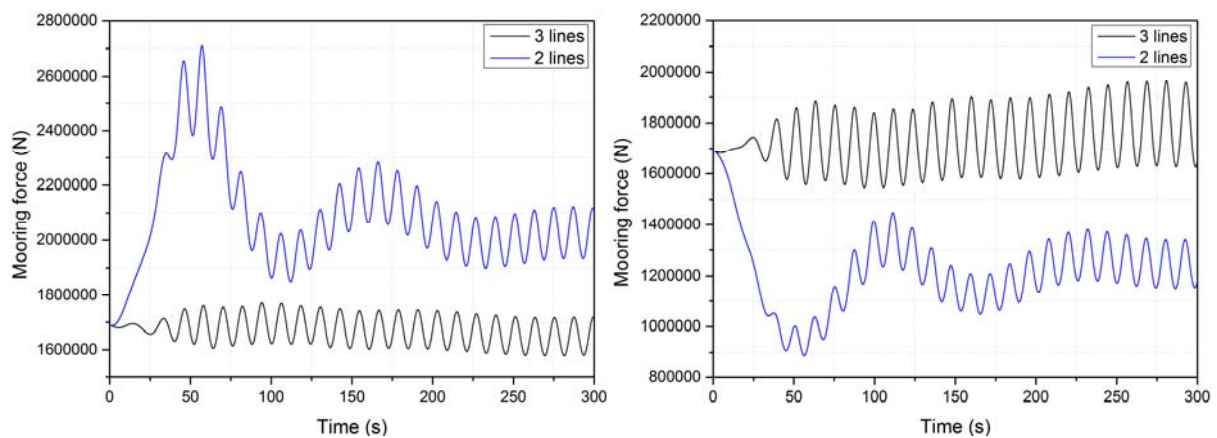


Figure 19. Position of the platform at 50 s and 0 s

In addition to the content above, the mooring forces of #1 and #2 are also investigated. As shown in the Figure 20, the blue line represents the one line broken condition and the other one represent the normal condition. It is easy to find that the mooring force of the #1 becomes larger after the #3 broken and the mooring force of #2 smaller. At the same time, the amplitude of the oscillation of the mooring force #1 becomes larger and the amplitude of #2 smaller in this procedure. All above analyses indicate that the load acting on mooring line #1 become larger and it plays a more significant role in the motion of the platform and the mooring system, and the #2 quite the contrary. So that it is the more dangerous one and more attention should be paid to the #1 when the #3 is broken.



(a) Mooring force of #1 line in two conditions

(b) Mooring force of #2 line in two conditions

Figure 20. Mooring force of #1 and #2 mooring line in these two conditions

Conclusion

In this paper, a viscous flow solver naoe-FOAM-SJTU based on the open source toolbox OpenFOAM is developed and presented. By comparing numerically calculated results with the experimental test data and the results of the FAST, the ability of present solver to handle hydrodynamic problems of floating structures with mooring system with various wave condition is validated. The solver is then adopted to investigate the parameter sensitive of the platform including the height of gravity center and the draft. In this section, several conclusion are drawn that the motion performance would be better with the decrease of the height of COG within a suitable range. Subsequently, it is found that the performance is better with the increase of the draft within a reasonable range. Moreover, to investigate the motion performance of the platform in a dangerous condition, one of the mooring line is removed to

simulate the condition that on mooring line is broken by the wave or flow force. Results indicates that the platform would move a certain distance along the direction against the x-axis and float up because of the lack of pretention force of the mooring line and cause the unbalanced force, as well the rotational movement. The mooring force of the rest two lines are investigated as well, which indicate that one of the two lines would be very generous whose mooring force increase immediately after the third line is broken. So that, people should pay more attention to this dangerous one in this condition. Although the present work are all based on the regular wave, the regular one can analyze the characteristic of the platform better, and the irregular wave would be carried out in the future work. The work done in this paper can serve as foundation for the design and working of the DeepCwind wind turbine platform which can ensure a more steady motion performance as well as the stability of the electricity generation. And the solver used in this paper can do more complex issues like VIV and wind-wave-current coupling issues in the future.

Acknowledgements

This work is supported by the National Natural Science Foundation of China (51379125, 51490675, 11432009, 51579145, 11272120), Chang Jiang Scholars Program (T2014099), Program for Professor of Special Appointment (Eastern Scholar) at Shanghai Institutions of Higher Learning (2013022), Innovative Special Project of Numerical Tank of Ministry of Industry and Information Technology of China (2016-23) and Lloyd's Register Foundation for doctoral student, to which the authors are most grateful.

References

- [1] MA, Y., Z. HU and L. XIAO, Wind-wave induced dynamic response analysis for motions and mooring loads of a spar-type offshore floating wind turbine. *Journal of Hydrodynamics, Ser. B*, 2015. 26(6): 865-874.
- [2] Tang, Y., K. Song and B. Wang, Experiment study of dynamics response for wind turbine system of floating foundation. *China Ocean Engineering*, 2015. 29(6): 835-846.
- [3] Zhao, Y., et al., Dynamic response analysis of a multi-column tension-leg-type floating wind turbine under combined wind and wave loading. *Journal of Shanghai Jiaotong University (Science)*, 2016. 21(1): 103-111.
- [4] Yang, H.Y.H.E., Optimization Design of TMD for Vibration Suppression of Offshore Floating Wind Turbine. *International Journal of Plant Engineering and Management*, 2015. 1(20): 13-27.
- [5] Hoof. Coupled Effects of Risers/Supporting Guide Frames on Spar Responses [A]. *Proc. 12th International Offshore and Polar Engineering Conf. [C]*, Kitakyushu, Japan, 2002: 231-236.
- [6] Lee Y W, Incecik A, Chan H S and Kim Z k. Design Evaluation in the Aspects of Hydrodynamics on a Prototype Semi-Submersible with Rectangular Cross-Section Members[A]. *Proceedings of the Fifteenth (2005) International Offshore and Polar Engineering Conference[C]*. Seoul, Korea, ISOPE2005: 320-327.
- [7] Frank, Lee D.Y., Choi Y.H., etc. An Experimental Study on the Extreme Motion Responses of a SPAR Platform in the Heave Resonant Waves [A]. *Proc. International Off-shore and Polar Engineering Conf. [C]*, Seoul, Korea, 2005: 225-232.
- [8] SHI Qi-qi, YANG Jian-min. Research on hydrodynamic characteristics of a semi-submersible platform and its mooring system. *The Ocean Engineering*, 2010. 28(4):1-8.
- [9] SHI Qi-qi, YANG Jian-min , XIAO Long-fei. Research on motion and hydrodynamic characteristics of a deepwater semi-submersible by numerical simulation and model test. *The Ocean Engineering*, 2011. 29(4):29-42.
- [10] Wang, S., et al., Hydrodynamic performance of a novel semi-submersible platform with nonsymmetrical pontoons. *Ocean Engineering*, 2015. 110: 106-115.
- [11] Yuanchuan Liu, Y.P.D.W., Numerical Investigation on Interaction between a Semi-submersible Platform and Its Mooring System. *Proceedings of the ASME 2015 34th International Conference on Ocean, Offshore and Arctic Engineering OMAE2015 May 31-June 5, 2015, St. John's, Newfoundland, Canada*.
- [12] Shen, Z. R., Zhao, W. W., Wang, J. H. and Wan, D. C. 2014. "Manual of CFD solver for ship and ocean engineering flows: naoe-FOAM-SJTU." Technical Report for Solver Manual, Shanghai Jiao Tong University.
- [13] A. Robertson, J. Jonkman, M. Masciola, H. Song, A. Goupee, A. Coulling, and C. Luan. Definition of the Semisubmersible Floating System for Phase II of OC4. 2012. Available from: <http://www.nrel.gov/>
- [14] Coulling, A.J., et al., Validation of a FAST semi-submersible floating wind turbine numerical model with DeepCwind test data. *Journal of Renewable and Sustainable Energy*, 2013. 5(2): 023116.
- [15] OpenFOAM. Mesh generation with the snappyHexMesh utility. 2013. Available from: <http://www.openfoam.org/docs/user/snappyHexMesh.php#x26-1510005.4>.